



Cs[Tf₂N]: a second polymorph with a layered structure

Jared T. Stritzinger,* Janelle E. Droessler, Brian L. Scott and George S. Goff

Materials Physics and Applications Division, Associate Directorate for Experimental Physical Sciences, Los Alamos National Laboratory, Los Alamos, New Mexico, 87545, USA. *Correspondence e-mail: jstritzinger@lanl.gov

Received 20 December 2017

Accepted 15 March 2018

Edited by M. Weil, Vienna University of Technology, Austria

Keywords: crystal structure; ionic liquid; bis-triflimide; layered structure.**CCDC reference:** 1830211**Supporting information:** this article has supporting information at journals.iucr.org/e

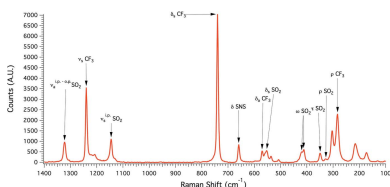
The structural determination of the ionic liquid, caesium bis[(trifluoromethyl)sulfonyl]imide or poly[[μ_4 -bis[(trifluoromethyl)sulfonyl]imido]caesium(I)], Cs[N(SO₂CF₃)₂] or Cs[Tf₂N], reveals a second polymorph that also crystallizes in a layer structure possessing monoclinic $P2_1/c$ symmetry at 120 K instead of $C2/c$ for the known polymorph [Xue *et al.* (2002). *Solid State Sci.* **4**, 1535–1545]. The caesium ions in the cationic layers are coordinated by the sulfonyl groups of the bistriflimide molecules from anion layers while the trifluoromethyl groups are oriented in the opposite direction, forming a non-polar surface separating the layers. The layer direction is (100).

1. Chemical context

Recently, ionic liquids (IL) with melting points below 373 K, known as room temperature ionic liquids (RTIL), have emerged as a novel system that can be used to replace processes utilizing hazardous organic solvents and provide water-free environments (Welton, 1999). The exclusion of water from RTIL can be challenging as their ionic nature predisposes a hygroscopic nature, and even so-called hydrophobic ILs can be difficult to dry (Francesco *et al.*, 2011). Reducing the solubility of water is possible by exchanging constituent ions of the IL for those that are less hydrophilic, but this often results in higher melting points or increased viscosity (Francesco *et al.*, 2011). The ability to change the physicochemical characteristics of ionic liquids has led them to be praised as ‘tunable solvents’, but is often more of a challenging act of balancing physical properties.

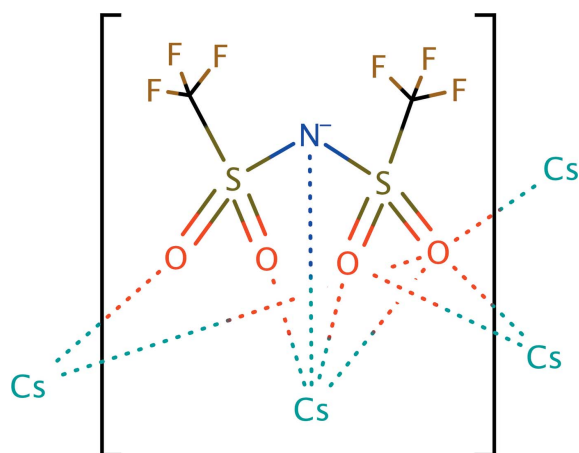
The substitution of bis(trifluoromethyl)sulfonyl)imide (bistriflimide, Tf₂N) as the anion in ILs offers a more hydrophobic IL with lower melting point (Matsumoto *et al.*, 2002; Sun *et al.*, 1997). In general, anions of the triflate family are weakly coordinating when in the presence of other ligands, and interactions with metal ions may not be observed when in the presence of water. These weak interactions are due to the delocalization of charge across the molecule. The structure of bistriflimide also allows for multidentate coordination motifs when binding through the oxygen atoms, and often results in coordination of multiple metal cations. When Tf₂N interactions expand beyond a single central metal atom, the ability to diffuse charge across a structure is highlighted (DesMar-teau, 1995).

Cs[Tf₂N] has a desirably low melting point of 398 K which is outside the conventional definition of a RTIL; however, this melting point is in the range of many well-known ILs while



still being above the boiling point of water to enable convenient drying (Hagiwara *et al.*, 2008; Scheuermeyer *et al.*, 2016). Previous reports of alkali metals and Tf_2N include $\text{Cs}[\text{Tf}_2\text{N}]$, which presents as either an anhydrate or a variety of hydrates (Xue *et al.*, 2002). Some common structural similarities can be observed across the $A[\text{Tf}_2\text{N}] \cdot n\text{H}_2\text{O}$ ($A = \text{Li}, \text{Na}, \text{K}, \text{Rb}, \text{and Cs}$) series. The most notable feature is the formation of polar and non-polar regions that result from the coordination of multiple metal cations by the Tf_2N^- ion. Each of the sulfonyl groups binds to a metal cation creating a polar chain that may extend to a layer, and orientates the trifluoromethyl groups to create non-polar surfaces. Within the series, only the structures of Cs and K salts as anhydrates have been reported.

Our synthesis and analysis of $\text{Cs}[\text{Tf}_2\text{N}]$ has revealed a second layered polymorph set in $P2_1/c$ in addition to the previously reported structure in $C2/c$ (Xue *et al.*, 2002).



2. Structural commentary

The structure develops from the various ways in which six Tf_2N molecules coordinate the central 10-coordinate caesium cation (Fig. 1). The simplest coordination mode is monodentate, where one oxygen atom on one of the sulfonyl groups of the Tf_2N molecule coordinates to the caesium cation. The bidentate coordination mode has two motifs. In end-on coordination, both oxygen atoms of a single sulfonyl group coordinate with Cs^+ , while in side-on coordination one oxygen on each of the sulfonyl groups within a Tf_2N molecule coordinate with Cs^+ . Two of the six distinct Tf_2N molecules exhibit the side-on coordination mode, and in one of them the nitrogen atom of the Tf_2N molecule may come close enough to interact with the caesium cation. Examining the bond lengths in the coordination environment of the caesium cation, it is comprised of nine oxygen atoms ranging from 3.060 (2)–3.539 (3) Å and one interaction with a nitrogen atom of 3.280 (3) Å. These three different modes of Tf_2N binding join the caesium cations together in a complex sheet with layers of trifluoromethyl groups above and below (Fig. 1).

As the Tf_2N molecule coordinates in the cis conformation, this orients the trifluoromethyl groups in the opposite direc-

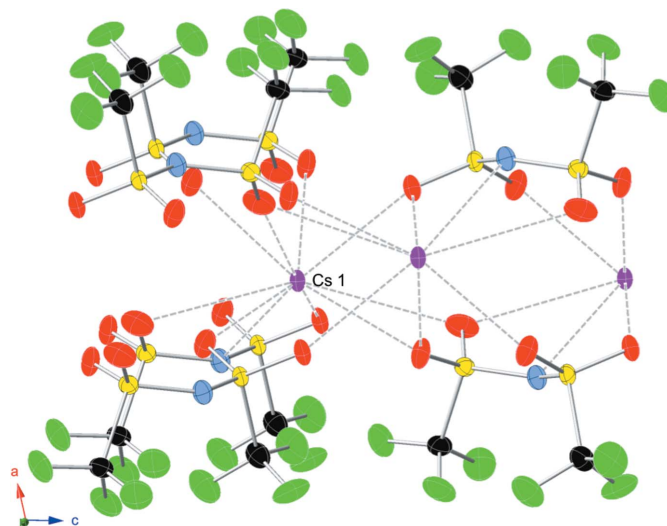
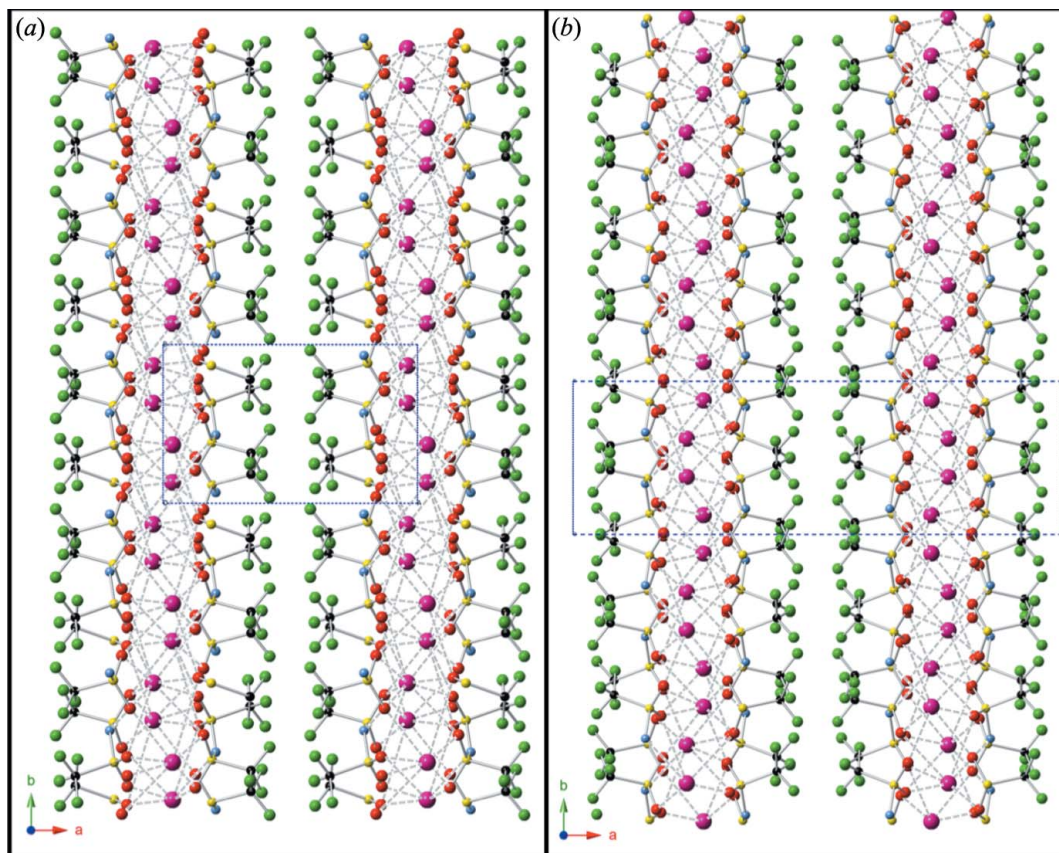


Figure 1

The coordination of the Cs^+ cation by nine oxygen atoms and one nitrogen atom of six different bistriflimide anions coordinating above and three below, in a view slightly off the (100) plane. Other caesium cations are crystallographically equivalent to $\text{Cs}1$, and are shown to depict how the sheet extends. The displacement ellipsoids are drawn at the 50% probability function with the color scheme of caesium (purple), oxygen (red), sulfur (yellow), nitrogen (blue), carbon (black), and fluorine (green).

tion from the sulfonyl groups creating a layer of fluorine atoms. With this layer, trifluoromethyl groups have an intramolecular closest contact of 2.770 (4) Å and an intermolecular closest contact of 2.970 (4) Å. There is a fluorine–fluorine closest contact length of 3.01 Å spanning the void between the non-polar surfaces of adjacent sheets in the layered structure. These layers are easily observed parallel to (100), Fig. 2. Examining the bistriflimide molecule, the S–N–S bond angle is 127.60 (17)° resulting in an intramolecular carbon–carbon separation of 4.18 Å.

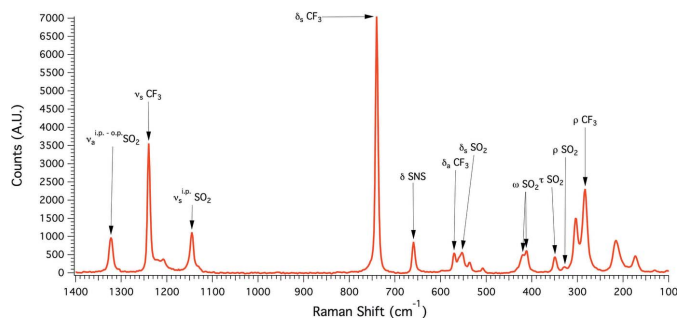
This structure of alternating layers of hydrophilic alkali metal cations bound by the sulfonyl groups and hydrophobic layers of trifluoromethyl groups closely matches the reported structures of $\text{K}[\text{Tf}_2\text{N}]$ and $\text{Cs}[\text{Tf}_2\text{N}]$ (Xue *et al.*, 2002). The noted deviations are in the coordination environment of the Cs^+ cation. For the previously reported structure of $\text{Cs}[\text{Tf}_2\text{N}]$, the caesium coordination environment is also 10; however, the oxygen interactions are generally longer by about 0.05 Å, with Cs–O bonds ranging from 3.04 (1) to 3.65 (1) Å. The lone Cs–N bond is 3.39 (1) Å, which is considerably longer than the 3.280 (3) Å bond length observed in the current structure. This extension of bond lengths is reflected in the bistriflimide molecule where the S–N–S bond angle is contracted to 126.38 and the intramolecular carbon–carbon separation is shortened to 4.08 Å. As the molecule shifts, so does the orientation of the trifluoromethyl groups, resulting in an intramolecular closest contact of 2.72 Å and an intermolecular closest contact of 2.96 Å. The shift also extends to the void between the non-polar surface of adjacent sheets, where fluorine–fluorine closest contacts are observed at 2.69 Å spanning the void. While the void space between layers


Figure 2

Ball and stick model view along [001] showing the layer of the structure arising from the hydrophobic surfaces formed by orientation of the trifluoromethyl groups, comparing (a) the unit cell of the structure discussed in the paper set in $P2_1/c$ and (b) that of the previously reported structure set in $C2/c$ (Xue *et al.*, 2002). Atoms are designated as caesium (purple), oxygen (red), sulfur (yellow), nitrogen (blue), carbon (black), and fluorine (green).

appears reduced, the overall structure has a calculated density of 2.58 g cm^{-3} (Xue *et al.*, 2002), less dense than the calculated 2.65 g cm^{-3} of the more compact current structure.

The $\text{Cs}[\text{Tf}_2\text{N}]$ purity was confirmed by melting point measurements that closely match literature values, showing an onset temperature of 397 K and complete melting at 399 K (Hagiwara *et al.*, 2008; Scheuermeyer *et al.*, 2016). Additional Raman analysis (Fig. 3), shows a number of features that


Figure 3

Raman spectra of $\text{Cs}[\text{Tf}_2\text{N}]$ with no other bands observed from 1400 cm^{-1} to 3200 cm^{-1} . The additional bands at 535 and 507 cm^{-1} suggest the multiple SO_2 bending modes associated with multiple coordination modes. Major band assignments are given with ν (stretching), δ (bending), ω (wagging), τ (twisting) and ρ (rocking) followed by the functional group. Planar designations are i.p. for in plane and o.p. for out of plane.

closely match the reported spectra for Tf_2N^- in water and solid-state measurements made on HTf_2N , confirming the presence of the Tf_2N molecule (Rey *et al.*, 1998). To elucidate bands that signify interactions with metal cations, a comparison to the reported Raman spectra of $\text{La}[\text{Tf}_2\text{N}]_3(\text{H}_2\text{O})_3$ (Bhatt *et al.*, 2005) was made. The major bands and assignments of all compounds in the comparisons are reported in Table 1. The additional bands observed at 535 and 507 cm^{-1} for $\text{Cs}[\text{Tf}_2\text{N}]$ suggest multiple SO_2 bending modes associated with multiple coordination modes of Tf_2N . In particular, the band at 507 cm^{-1} for $\text{Cs}[\text{Tf}_2\text{N}]$ matches with a 511 cm^{-1} band in $\text{La}[\text{Tf}_2\text{N}]_3(\text{H}_2\text{O})_3$ suggesting a tentative assignment to a down-shift of the SO_2 bending mode by the bidentate side-on coordination of the Tf_2N molecule, observed in both structures.

3. Synthesis and crystallization

All reagents were used as received without further purification. 20.281 g of caesium carbonate (Alfa Aesar, 99.9%) were dissolved in 20 ml of deionized water. 26.26 ml of 4.74 molar bistriflimide acid (Alfa Aesar, 98.0%) were slowly added to the caesium carbonate solution, resulting in vigorous release of carbon dioxide. The solution was then placed in a sand bath at 403 K under stirring at approximately 100 rotations per

Table 1

Comparison of Raman modes in Tf_2N compounds.

Comparison of observed Raman shifts in cm^{-1} from Tf_2N -containing compounds. Band wavenumbers given in bold are unassigned and in italicized are from reanalysis of reported spectra for $\text{La}[\text{Tf}_2\text{N}]_3(\text{H}_2\text{O})_3$. Major band assignments are given with ν (stretching), δ (bending), ω (wagging), τ (twisting) and ρ (rocking) and planar designations are i.p. for in plane and o.p. for out of plane.

Mode	Group	Tf_2N^- in H_2O	HTf_2N	$\text{La}[\text{Tf}_2\text{N}]_3(\text{H}_2\text{O})_3$	$\text{Cs}[\text{Tf}_2\text{N}]$
			1456		
			1443		
ν_a i.p.	SO_2	1351			
ν_a o.p.	SO_2	1332	1436	1316	1322
			1427		
δ	NH		1332		
ν_s	CF_3	1239	1250	1243	1240
ν_a	CF_3		1220		
		1203	1208	1210	1206
ν_s i.p.	SO_2	1131	1134	1148	1145
δ_s	CF_3	744	765	754	740
δ	SNS		634	669	659
δ_a i.p.	SO_2	594	583		
δ_a	CF_3	567	570	573	572
			555		
δ_s	SO_2	551		554	553
				535	535
				511	507
γ	NH		526		
			495	444	
ω	SO_2	407, 401			420, 412
			380		
τ	SO_2	351		356	349
		339			
ρ	SO_2	325	335	332	328
		312	299	310	304
ν	MO			297?	
ρ	CF_3	276		288	283
			264	241	
			210		215
			202		173
			185		130

minute. After four h, the temperature was reduced to 378 K. While the liquid cooled, the stirring deposited droplets of the ionic liquid on the sides of the beaker resulting in rapid crystallization. These crystals were harvested and suitable crystals were selected for diffraction. Yield was estimated at 95% based on mass.

3.1. Experimental

Raman measurements were collected using a Thermo Scientific DXRxi Raman Imaging Microscope. A 532 nm laser was focused on the sample surface through a 10x objective providing a spot size of 1 μm and the collection consisted of 200 scans at 10 mW for 0.25 seconds each.

Melting point data were collected on a Büchi M-560, where two glass sample tubes were filled with 4–5 mm of sample and the temperature was ramped at a rate of 0.5 K per minute.

4. Refinement

Crystal data, data collection and structure refinement details are summarized in Table 2.

Table 2

Experimental details.

Crystal data	
Chemical formula	$[\text{Cs}(\text{C}_2\text{F}_6\text{NO}_4\text{S}_2)]$
M_r	413.06
Crystal system, space group	Monoclinic, $P2_1/c$
Temperature (K)	120
a, b, c (Å)	11.431 (4), 6.918 (2), 13.469 (4)
β (°)	103.686 (4)
V (Å ³)	1035.0 (5)
Z	4
Radiation type	Mo $K\alpha$
μ (mm ⁻¹)	4.07
Crystal size (mm)	0.40 × 0.35 × 0.33
Data collection	
Diffractometer	Bruker Photon 100
Absorption correction	Multi-scan (SADABS; Bruker, 2014)
$T_{\text{min}}, T_{\text{max}}$	0.507, 0.746
No. of measured, independent and observed [$I > 2\sigma(I)$] reflections	12467, 2354, 1980
R_{int}	0.048
$(\sin \theta/\lambda)_{\text{max}}$ (Å ⁻¹)	0.650
Refinement	
$R[F^2 > 2\sigma(F^2)], wR(F^2), S$	0.022, 0.058, 0.99
No. of reflections	2354
No. of parameters	145
$\Delta\rho_{\text{max}}, \Delta\rho_{\text{min}}$ (e Å ⁻³)	0.84, -1.15

Computer programs: APEX2 (Bruker, 2014), SAINT-Plus (Bruker, 2014), SHELXT2014 (Sheldrick, 2015a), SHELXL2014 (Sheldrick, 2015b), CrystalMaker (CrystalMaker, 2013).

Funding information

Funding for this research was provided by: National Nuclear Security Administration (NA-23).

References

- Bhatt, A. I., May, I., Volkovich, V. A., Collison, D., Helliwell, M., Polovov, I. B. & Lewin, R. G. (2005). *Inorg. Chem.* **44**, 4934–4940.
- Bruker (2014). APEX2, SAINT-Plus and SADABS. Bruker AXS Inc., Madison, Wisconsin, USA.
- CrystalMaker (2013). *CrystalMaker*. CrystalMaker Software, Oxfordshire, UK.
- DesMarteau, D. D. (1995). *J. Fluor. Chem.* **72**, 203–208.
- Francesco, F. D., Calisi, N., Creatini, M., Melai, B., Salvo, P. & Chiappe, C. (2011). *Green Chem.* **13**, 1712–1717.
- Hagiwara, R., Tamaki, K., Kubota, K., Goto, T. & Nohira, T. (2008). *J. Chem. Eng. Data*, **53**, 355–358.
- Matsumoto, H., Kageyama, H. & Miyazaki, Y. (2002). *Chem. Commun.* pp. 1726–1727.
- Rey, I., Johansson, P., Lindgren, J., Lassègues, J. C., Grondin, J. & Servant, L. (1998). *J. Phys. Chem. A*, **102**, 3249–3258.
- Scheuermeyer, M., Kusche, M., Agel, F., Schreiber, P., Maier, F., Steinrück, H.-P., Davis, J. H., Heym, F., Jess, A. & Wasserscheid, P. (2016). *New J. Chem.* **40**, 7157–7161.
- Sheldrick, G. M. (2015a). *Acta Cryst.* **A71**, 3–8.
- Sheldrick, G. M. (2015b). *Acta Cryst.* **C71**, 3–8.
- Sun, J., MacFarlane, D. R. & Forsyth, M. (1997). *Ionics*, **3**, 356–362.
- Welton, T. (1999). *Chem. Rev.* **99**, 2071–2084.
- Xue, L., Padgett, C. W., DesMarteau, D. D. & Pennington, W. T. (2002). *Solid State Sci.* **4**, 1535–1545.

supporting information

Acta Cryst. (2018). E74, 551-554 [https://doi.org/10.1107/S2056989018004401]

Cs[Tf₂N]: a second polymorph with a layered structure

Jared T. Stritzinger, Janelle E. Droessler, Brian L. Scott and George S. Goff

Computing details

Data collection: *APEX2* (Bruker, 2014); cell refinement: *SAINTE-Plus* (Bruker, 2014); data reduction: *SAINTE-Plus* (Bruker, 2014); program(s) used to solve structure: *SHELXT2014* (Sheldrick, 2015a); program(s) used to refine structure: *SHELXL2014* (Sheldrick, 2015b); molecular graphics: *CrystalMaker* (*CrystalMaker*, 2013); software used to prepare material for publication: *SHELXL2014* (Sheldrick, 2015b).

Poly[[μ_4 -bis[(trifluoromethyl)sulfonyl]imido]caesium(I)]

Crystal data

[Cs(C₂F₆NO₄S₂)]

$M_r = 413.06$

Monoclinic, *P2₁/c*

$a = 11.431$ (4) Å

$b = 6.918$ (2) Å

$c = 13.469$ (4) Å

$\beta = 103.686$ (4)°

$V = 1035.0$ (5) Å³

$Z = 4$

$F(000) = 768$

$D_x = 2.651$ Mg m⁻³

Melting point: 399 K

Mo $K\alpha$ radiation, $\lambda = 0.71073$ Å

Cell parameters from 12467 reflections

$\theta = 3.1$ – 27.5 °

$\mu = 4.07$ mm⁻¹

$T = 120$ K

Block, colorless

$0.40 \times 0.35 \times 0.33$ mm

Data collection

Bruker Photon 100
diffractometer

Radiation source: sealed tube

Detector resolution: 0 pixels mm⁻¹

0.5 wide w/exposures scans

Absorption correction: multi-scan
(*SADABS*; Bruker, 2014)

$T_{\min} = 0.507$, $T_{\max} = 0.746$

12467 measured reflections

2354 independent reflections

1980 reflections with $I > 2\sigma(I)$

$R_{\text{int}} = 0.048$

$\theta_{\max} = 27.5$ °, $\theta_{\min} = 3.1$ °

$h = -14 \rightarrow 14$

$k = -8 \rightarrow 8$

$l = -17 \rightarrow 17$

Refinement

Refinement on F^2

Least-squares matrix: full

$R[F^2 > 2\sigma(F^2)] = 0.022$

$wR(F^2) = 0.058$

$S = 0.99$

2354 reflections

145 parameters

0 restraints

$w = 1/[\sigma^2(F_o^2) + (0.0256P)^2 + 1.4815P]$

where $P = (F_o^2 + 2F_c^2)/3$

$(\Delta/\sigma)_{\max} = 0.001$

$\Delta\rho_{\max} = 0.84$ e Å⁻³

$\Delta\rho_{\min} = -1.15$ e Å⁻³

Special details

Experimental. Single crystal data for [Cs][Tf₂N] were collected on a Bruker D8 Quest diffractometer, with CMOS detector in shutterless mode. The crystal was cooled to 100 K employing an Oxford Cryostream liquid nitrogen cryostat. The diffractometer was equipped with graphite monochromatized MoK α ($\lambda = 0.71073$ Å) radiation. A hemisphere of data was collected using omega scans and 0.5° frame widths. Data collection and initial indexing and cell refinement were handled using APEX III (Bruker, 2014) software. Frame integration, including Lorentz-polarization corrections, and final cell parameter calculations were carried out using SAINT+ software (Bruker, 2014). The data were corrected for absorption using redundant reflections and the SADABS (Bruker, 2014) program. Decay of reflection intensity was not observed as monitored *via* analysis of redundant frames. The structure was solved using Direct methods and difference Fourier techniques.

Geometry. All esds (except the esd in the dihedral angle between two l.s. planes) are estimated using the full covariance matrix. The cell esds are taken into account individually in the estimation of esds in distances, angles and torsion angles; correlations between esds in cell parameters are only used when they are defined by crystal symmetry. An approximate (isotropic) treatment of cell esds is used for estimating esds involving l.s. planes.

Fractional atomic coordinates and isotropic or equivalent isotropic displacement parameters (Å²)

	<i>x</i>	<i>y</i>	<i>z</i>	<i>U</i> _{iso} */ <i>U</i> _{eq}
Cs1	−0.03866 (2)	0.63206 (3)	0.14267 (2)	0.01618 (7)
S1	−0.19100 (7)	1.13281 (11)	0.03845 (6)	0.01796 (16)
S2	−0.19461 (7)	0.61691 (11)	0.37165 (6)	0.01711 (16)
F3	−0.3349 (2)	1.3866 (4)	0.0842 (2)	0.0490 (7)
O1	−0.1407 (2)	1.0987 (4)	0.14485 (18)	0.0335 (6)
F6	−0.4204 (2)	0.5355 (4)	0.29152 (18)	0.0473 (7)
F2	−0.4023 (2)	1.0936 (4)	0.0776 (2)	0.0523 (7)
F1	−0.4044 (2)	1.2485 (4)	−0.06094 (18)	0.0451 (6)
F5	−0.3425 (2)	0.7475 (4)	0.21036 (16)	0.0419 (6)
O4	−0.1614 (2)	0.4598 (4)	0.31460 (17)	0.0282 (6)
F4	−0.3890 (2)	0.8228 (4)	0.3522 (2)	0.0512 (7)
N1	−0.2092 (3)	0.5687 (4)	0.48229 (19)	0.0198 (6)
O2	−0.1390 (2)	1.2826 (4)	−0.01035 (19)	0.0301 (6)
O3	−0.1285 (2)	0.7926 (4)	0.3755 (2)	0.0355 (6)
C2	−0.3470 (3)	0.6835 (6)	0.3026 (3)	0.0286 (8)
C1	−0.3433 (3)	1.2186 (5)	0.0345 (3)	0.0284 (8)

Atomic displacement parameters (Å²)

	<i>U</i> ¹¹	<i>U</i> ²²	<i>U</i> ³³	<i>U</i> ¹²	<i>U</i> ¹³	<i>U</i> ²³
Cs1	0.02257 (12)	0.01463 (11)	0.01149 (10)	−0.00018 (7)	0.00432 (7)	0.00054 (7)
S1	0.0186 (4)	0.0238 (4)	0.0111 (3)	−0.0036 (3)	0.0026 (3)	−0.0028 (3)
S2	0.0171 (4)	0.0168 (4)	0.0171 (4)	−0.0003 (3)	0.0035 (3)	0.0026 (3)
F3	0.0498 (15)	0.0461 (15)	0.0501 (15)	0.0090 (12)	0.0098 (12)	−0.0265 (12)
O1	0.0318 (14)	0.0543 (17)	0.0119 (11)	0.0032 (13)	0.0004 (10)	−0.0044 (11)
F6	0.0293 (13)	0.0630 (17)	0.0413 (14)	−0.0197 (12)	−0.0084 (10)	0.0121 (12)
F2	0.0309 (13)	0.0638 (18)	0.0702 (19)	−0.0044 (12)	0.0278 (13)	0.0039 (14)
F1	0.0422 (14)	0.0450 (14)	0.0385 (13)	0.0177 (11)	−0.0094 (11)	−0.0069 (11)
F5	0.0439 (14)	0.0521 (15)	0.0249 (11)	0.0025 (12)	−0.0017 (10)	0.0189 (11)
O4	0.0422 (15)	0.0271 (13)	0.0193 (12)	0.0111 (11)	0.0157 (11)	0.0058 (10)
F4	0.0458 (15)	0.0580 (16)	0.0496 (15)	0.0322 (13)	0.0103 (12)	0.0048 (13)

N1	0.0249 (15)	0.0184 (13)	0.0154 (13)	0.0017 (11)	0.0034 (11)	-0.0029 (10)
O2	0.0414 (15)	0.0269 (13)	0.0266 (13)	-0.0148 (11)	0.0170 (11)	-0.0097 (10)
O3	0.0315 (15)	0.0251 (13)	0.0462 (16)	-0.0104 (11)	0.0019 (12)	0.0091 (12)
C2	0.0229 (18)	0.0355 (19)	0.0259 (18)	0.0031 (15)	0.0029 (14)	0.0092 (15)
C1	0.0284 (19)	0.0291 (19)	0.0257 (18)	0.0036 (15)	0.0022 (15)	-0.0061 (14)

Geometric parameters (Å, °)

Cs1—O2 ⁱ	3.060 (2)	S2—N1	1.574 (3)
Cs1—O3 ⁱⁱ	3.074 (3)	S2—C2	1.829 (4)
Cs1—O1 ⁱⁱ	3.110 (2)	S2—Cs1 ^{vii}	4.0548 (12)
Cs1—O4 ⁱⁱⁱ	3.174 (3)	F3—C1	1.333 (4)
Cs1—O2 ^{iv}	3.208 (2)	F3—Cs1 ^{vi}	3.703 (3)
Cs1—O4	3.207 (2)	O1—Cs1 ⁱⁱⁱ	3.110 (2)
Cs1—N1 ^v	3.280 (3)	F6—C2	1.310 (5)
Cs1—O1	3.435 (3)	F2—C1	1.314 (5)
Cs1—O3 ^v	3.539 (3)	F1—C1	1.326 (4)
Cs1—O3	3.694 (3)	F5—C2	1.331 (4)
Cs1—F3 ^{iv}	3.703 (3)	O4—Cs1 ⁱⁱ	3.175 (3)
Cs1—S2	3.9118 (12)	F4—C2	1.326 (5)
S1—O1	1.432 (2)	N1—S1 ^{vii}	1.576 (3)
S1—O2	1.430 (3)	N1—Cs1 ^{vii}	3.280 (3)
S1—N1 ^v	1.576 (3)	O2—Cs1 ⁱ	3.060 (2)
S1—C1	1.828 (4)	O2—Cs1 ^{vi}	3.208 (2)
S1—Cs1 ^{vi}	3.9719 (12)	O3—Cs1 ⁱⁱⁱ	3.074 (3)
S2—O3	1.426 (3)	O3—Cs1 ^{vii}	3.539 (3)
S2—O4	1.433 (2)		
O2 ⁱ —Cs1—O3 ⁱⁱ	65.81 (8)	O3—Cs1—S2	21.36 (4)
O2 ⁱ —Cs1—O1 ⁱⁱ	99.58 (7)	F3 ^{iv} —Cs1—S2	65.85 (4)
O3 ⁱⁱ —Cs1—O1 ⁱⁱ	74.33 (7)	O1—S1—O2	117.87 (17)
O2 ⁱ —Cs1—O4 ⁱⁱⁱ	54.48 (6)	O1—S1—N1 ^v	108.10 (16)
O3 ⁱⁱ —Cs1—O4 ⁱⁱⁱ	97.22 (8)	O2—S1—N1 ^v	116.27 (14)
O1 ⁱⁱ —Cs1—O4 ⁱⁱⁱ	66.20 (7)	O1—S1—C1	103.70 (16)
O2 ⁱ —Cs1—O2 ^{iv}	87.52 (7)	O2—S1—C1	104.35 (17)
O3 ⁱⁱ —Cs1—O2 ^{iv}	60.48 (7)	N1 ^v —S1—C1	104.86 (16)
O1 ⁱⁱ —Cs1—O2 ^{iv}	126.37 (7)	O1—S1—Cs1 ^{vi}	75.58 (12)
O4 ⁱⁱⁱ —Cs1—O2 ^{iv}	141.95 (6)	O2—S1—Cs1 ^{vi}	48.47 (10)
O2 ⁱ —Cs1—O4	162.97 (7)	N1 ^v —S1—Cs1 ^{vi}	159.36 (11)
O3 ⁱⁱ —Cs1—O4	99.20 (7)	C1—S1—Cs1 ^{vi}	93.60 (12)
O1 ⁱⁱ —Cs1—O4	67.27 (7)	O1—S1—Cs1	57.66 (12)
O4 ⁱⁱⁱ —Cs1—O4	123.62 (5)	O2—S1—Cs1	126.74 (12)
O2 ^{iv} —Cs1—O4	91.89 (7)	N1 ^v —S1—Cs1	52.89 (10)
O2 ⁱ —Cs1—N1 ^v	82.39 (7)	C1—S1—Cs1	128.83 (13)
O3 ⁱⁱ —Cs1—N1 ^v	135.52 (7)	Cs1 ^{vi} —S1—Cs1	120.90 (3)
O1 ⁱⁱ —Cs1—N1 ^v	144.35 (7)	O3—S2—O4	117.41 (17)
O4 ⁱⁱⁱ —Cs1—N1 ^v	87.65 (7)	O3—S2—N1	108.66 (16)
O2 ^{iv} —Cs1—N1 ^v	89.20 (7)	O4—S2—N1	116.61 (14)

O4—Cs1—N1 ^v	114.62 (7)	O3—S2—C2	103.71 (17)
O2 ⁱ —Cs1—O1	95.58 (7)	O4—S2—C2	105.06 (17)
O3 ⁱⁱ —Cs1—O1	159.64 (7)	N1—S2—C2	103.49 (16)
O1 ⁱⁱ —Cs1—O1	102.31 (7)	O3—S2—Cs1	70.70 (12)
O4 ⁱⁱⁱ —Cs1—O1	63.81 (7)	O4—S2—Cs1	50.92 (10)
O2 ^{iv} —Cs1—O1	130.03 (7)	N1—S2—Cs1	157.27 (11)
O4—Cs1—O1	97.80 (6)	C2—S2—Cs1	98.57 (12)
N1 ^v —Cs1—O1	42.47 (6)	O3—S2—Cs1 ^{vii}	59.03 (12)
O2 ⁱ —Cs1—O3 ^v	56.78 (7)	O4—S2—Cs1 ^{vii}	133.75 (11)
O3 ⁱⁱ —Cs1—O3 ^v	93.89 (6)	N1—S2—Cs1 ^{vii}	50.27 (10)
O1 ⁱⁱ —Cs1—O3 ^v	156.36 (7)	C2—S2—Cs1 ^{vii}	120.87 (13)
O4 ⁱⁱⁱ —Cs1—O3 ^v	95.87 (6)	Cs1—S2—Cs1 ^{vii}	120.87 (3)
O2 ^{iv} —Cs1—O3 ^v	58.95 (7)	C1—F3—Cs1 ^{vi}	117.4 (2)
O4—Cs1—O3 ^v	135.86 (7)	S1—O1—Cs1 ⁱⁱⁱ	158.44 (17)
N1 ^v —Cs1—O3 ^v	41.69 (6)	S1—O1—Cs1	101.72 (13)
O1—Cs1—O3 ^v	81.53 (6)	Cs1 ⁱⁱⁱ —O1—Cs1	85.77 (6)
O2 ⁱ —Cs1—O3	142.43 (6)	S2—O4—Cs1 ⁱⁱ	135.68 (14)
O3 ⁱⁱ —Cs1—O3	126.88 (6)	S2—O4—Cs1	108.79 (12)
O1 ⁱⁱ —Cs1—O3	59.74 (7)	Cs1 ⁱⁱ —O4—Cs1	88.69 (6)
O4 ⁱⁱⁱ —Cs1—O3	87.95 (6)	S2—N1—S1 ^{vii}	127.60 (17)
O2 ^{iv} —Cs1—O3	130.02 (6)	S2—N1—Cs1 ^{vii}	108.07 (13)
O4—Cs1—O3	40.70 (6)	S1 ^{vii} —N1—Cs1 ^{vii}	104.58 (12)
N1 ^v —Cs1—O3	97.36 (7)	S1—O2—Cs1 ⁱ	144.39 (15)
O1—Cs1—O3	63.07 (6)	S1—O2—Cs1 ^{vi}	112.04 (12)
O3 ^v —Cs1—O3	138.32 (6)	Cs1 ⁱ —O2—Cs1 ^{vi}	92.48 (7)
O2 ⁱ —Cs1—F3 ^{iv}	131.63 (6)	S2—O3—Cs1 ⁱⁱⁱ	169.31 (18)
O3 ⁱⁱ —Cs1—F3 ^{iv}	100.78 (7)	S2—O3—Cs1 ^{vii}	100.76 (13)
O1 ⁱⁱ —Cs1—F3 ^{iv}	122.16 (7)	Cs1 ⁱⁱⁱ —O3—Cs1 ^{vii}	86.11 (6)
O4 ⁱⁱⁱ —Cs1—F3 ^{iv}	161.69 (6)	S2—O3—Cs1	87.94 (13)
O2 ^{iv} —Cs1—F3 ^{iv}	49.29 (6)	Cs1 ⁱⁱⁱ —O3—Cs1	81.90 (6)
O4—Cs1—F3 ^{iv}	56.56 (7)	Cs1 ^{vii} —O3—Cs1	146.66 (8)
N1 ^v —Cs1—F3 ^{iv}	77.18 (7)	F6—C2—F5	108.6 (3)
O1—Cs1—F3 ^{iv}	97.90 (6)	F6—C2—F4	109.1 (3)
O3 ^v —Cs1—F3 ^{iv}	79.67 (6)	F5—C2—F4	109.1 (3)
O3—Cs1—F3 ^{iv}	83.94 (6)	F6—C2—S2	111.6 (3)
O2 ⁱ —Cs1—S2	162.46 (5)	F5—C2—S2	108.4 (2)
O3 ⁱⁱ —Cs1—S2	116.76 (6)	F4—C2—S2	110.0 (3)
O1 ⁱⁱ —Cs1—S2	66.21 (6)	F2—C1—F1	108.9 (3)
O4 ⁱⁱⁱ —Cs1—S2	108.62 (4)	F2—C1—F3	109.5 (3)
O2 ^{iv} —Cs1—S2	109.03 (5)	F1—C1—F3	108.0 (3)
O4—Cs1—S2	20.30 (5)	F2—C1—S1	111.0 (3)
N1 ^v —Cs1—S2	103.02 (5)	F1—C1—S1	111.0 (3)
O1—Cs1—S2	78.43 (4)	F3—C1—S1	108.3 (3)
O3 ^v —Cs1—S2	136.79 (5)		

Symmetry codes: (i) $-x, -y+2, -z$; (ii) $-x, y-1/2, -z+1/2$; (iii) $-x, y+1/2, -z+1/2$; (iv) $x, y-1, z$; (v) $x, -y+3/2, z-1/2$; (vi) $x, y+1, z$; (vii) $x, -y+3/2, z+1/2$.